frontiers | Frontiers in Energy Research

TYPE Original Research
PUBLISHED 01 September 2023
DOI 10.3389/fenrg.2023.1259067

OPEN ACCESS

EDITED BY
Shiwei Xie,
Fuzhou University, China

REVIEWED BY
Tomasz Górski,
University of Gdansk, Poland
Lv Chaoxian,
China University of Mining and Technology, China

*CORRESPONDENCE
Tao Yu,
taoyu1@scut.edu.cn

RECEIVED 15 July 2023
ACCEPTED 14 August 2023
PUBLISHED 01 September 2023

CITATION
Huan J, Ding Q, Yu T and Cheng Y (2023), Multi-stage low-carbon planning of an integrated energy system considering demand response.
Front. Energy Res. 11:1259067.
doi: 10.3389/fenrg.2023.1259067

Multi-stage low-carbon planning of an integrated energy system considering demand response

Jiajia Huan[1], Qiaoyi Ding[2], Tao Yu[2]* and Yusi Cheng[2]

[1]Guangdong Power Grid Co., Ltd., Guangzhou, China, [2]School of Electric Power Engineering, South China University of Technology, Guangzhou, China

In the context of energy crisis, the development of low-carbon integrated energy systems has become a prominent research area. This article addresses the challenges posed by high energy consumption and emissions in integrated energy systems by proposing a multi-stage planning method for low-carbon integrated energy that considers load time transfer characteristics. The first step involves examining the time transfer characteristics of demand response and analyzing the economic benefits of integrated energy systems participating in the electricity–carbon market. Subsequently, a multi-stage green low-carbon planning model for the integrated energy system is constructed. To validate the effectiveness of the proposed model, actual calculation results are obtained. These results demonstrate that the demand response, specifically in data centers, can significantly reduce the operational costs of integrated energy systems. Furthermore, the multi-stage low-carbon planning approach is shown to be more reasonable and economically beneficial compared to single-stage planning. Overall, this research article provides insights into the development of low-carbon integrated energy systems within the context of energy crisis. By considering load time transfer characteristics and employing a multi-stage planning method, this article highlights the potential for reducing costs and improving the overall efficiency of integrated energy systems.

KEYWORDS

integrated energy systems, multi-stage planning, low-carbon planning, data center, demand response

1 Introduction

With the energy crisis becoming increasingly serious (Yang L. et al., 2022), energy conservation and low-carbon development have gradually become the development philosophy of all countries in the world. The integrated energy system can achieve multi-energy coupling, improve the consumption rate of renewable energy through electricity–gas–thermal complementarity, and reduce carbon emissions. It is an important means to achieve carbon emission reduction goals. Therefore, it has received widespread attention from countries around the world (Lv et al., 2021). Therefore, in the context of green and low-carbon development, this article focuses on the planning of integrated energy systems and conducts research on multi-stage green and low-carbon comprehensive energy planning considering carbon emissions, providing theoretical and technical support for relevant researchers and planners.

2 Related work

At present, there are relatively mature research studies on the planning of integrated energy systems that consider carbon emissions, but the impact of the electricity–carbon market has not been fully considered in the planning. Chen et al. (2021) constructed a multi-stage planning method for the integrated energy system under a tiered carbon trading mechanism. Zhang et al. (2015) proposed a planning scheme that considers reliability, energy efficiency, and carbon emissions for the expansion plan of the electrical thermal coupling integrated energy hub. Xiong et al. (2021) studied the optimal configuration of hydrogen energy storage based on the electrical thermal load characteristics of integrated energy systems and verified its feasibility of reducing energy supply costs and carbon emissions. Li et al. (1608) proposed a low-carbon operation optimization strategy considering the electricity gas thermal hydrogen demand response and stepped carbon emission costs. Yuan et al. (2023) studied the optimization and scheduling method of integrated energy at the park level under the carbon green certificate trading mechanism. Zhang et al. (2020) introduced a reward and punishment tiered carbon trading mechanism to address the collaborative planning problem of integrated energy systems, taking into account the uncertainty of electric heating flexible loads, and proposed an integrated energy system planning model. Luo et al. (2021) constructed an integrated energy optimization scheduling model for the carbon green certificate joint trading mechanism, which can effectively improve the consumption rate of renewable energy. Liu et al. (2023) proposed dual-level optimization scheduling of integrated energy that considers carbon emission flow and demand side response to address the issue of low-carbon scheduling of integrated energy, which can achieve low-carbon economic operation. Qiu et al. (2015a) introduced a carbon trading mechanism and constructed an electricity gas joint expansion planning model that considers both economic and low-carbon aspects. Wang et al. (2019) proposed an optimal-capacity allocation model for the integrated energy system in the park, effectively improving the consumption rate of renewable energy and reducing carbon emissions. Shen et al. (2020) proposed data-driven robust planning for industrial integrated energy systems in response to various uncertainties. Zeng et al. (2023) proposed a double-layer optimization model based on the improved non-dominated sorting genetic algorithm-II (NSGA-II) and mixed-integer linear programming (MILP). Zhang et al. (2023) proposed a low-carbon economic dispatch model for an integrated energy system that considers an LCES and carbon capture system. The aforementioned literature conducted in-depth research on the low-carbon operation planning of integrated energy systems, but did not consider the impact of electricity markets on the power balance of integrated energy systems.

Many scholars have conducted multi-stage planning research on the planning of integrated energy systems. Zhao et al. (2020) constructed a long-term planning method for the integrated energy system of a park that takes into account the uncertainty of wind, light, and load. Wei et al. (2022) proposed a multi-objective extended planning model for the integrated energy system of electricity gas interconnection based on IGDT to address the problem of load fluctuations in the electricity gas system. Cao et al. (2020) proposed a multi-stage integrated energy system planning model to address the shortcomings of single-phase construction issues. Chen et al. (2022) constructed a dual-layer optimization configuration model for PIES that considers optimal construction timing and cloud energy storage. This model can improve the planning economy and equipment utilization efficiency of PIES. Qiu et al. (2015b) considered the uncertainty of load and cost and proposed multi-stage planning for a typical scenario based on an electric pneumatic coupling integrated energy system. Santos et al. (2015) proposed a multi-stage distributed generation planning model considering short-term and medium- and long-term uncertainties. Unsihuay-Vila et al. (2010) proposed an expansion model for a multi-region and multi-stage integrated energy system with electricity and gas coupling. Ding et al. (2018) proposed a multi-stage stochastic programming model for the electricity gas integrated energy system based on "wait-and-see decision-making" in response to load uncertainty. However, the aforementioned literature did not conduct research on how to achieve multi-stage energy structure transformation of the integrated energy system while meeting carbon emission reduction goals.

3 Discussion and limitations

In summary, the current research has not fully considered the impact of the electricity–carbon market, and the constraints of different carbon reduction goals on the planning of the integrated energy system were omitted. The time transfer characteristics of demand response, such as data centers in the integrated energy system, were overlooked. In addition, existing multi-stage planning methods lack consideration for the exchange of information among various components of the integrated energy system, and different components are in a relatively fragmented state, which cannot coordinate planning and operation well to achieve economic optimal results (Zhao Ning et al., 2023; Gorski, 2023).

Therefore, this article considers the time transfer characteristics of data center servers and electric refrigerators, studies the optimal timing of energy equipment construction, and constructs a low-carbon multi-stage planning model of an integrated energy system considering carbon neutrality paths. A low-carbon integrated energy system planning model with the goal of minimizing comprehensive costs is proposed. It is converted into mixed-integer linear programming and solved by Gurobi. Finally, the effectiveness of the proposed model is verified by the results of practical examples.

This article is mainly divided into four parts. The first part constructs the overall framework of the integrated energy system, clarifying the main energy types, energy equipment types, and load types included in the integrated energy system. The second part studies the time transfer characteristic of the demand response and constructs adjustable models for servers and electric refrigerators. The third part constructs the income model of integrated energy in the electricity–carbon market. The electricity market considers the income of the day-ahead electricity market and the day-ahead frequency modulation market, and the carbon market considers the economic income under the stepped carbon trading mechanism. The fourth part is example verification.

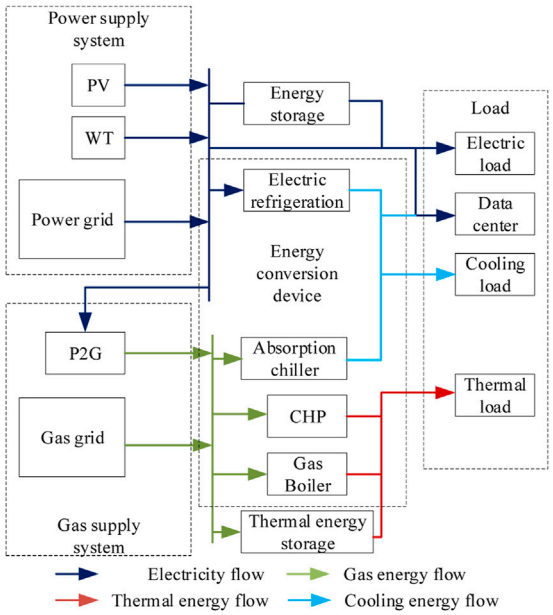

FIGURE 1
Integrated energy system structure.

4 Structure of the integrated energy system

The structure of the integrated energy system in this article is shown in Figure 1. The energy supply side of the integrated energy system includes the superior power grid, natural gas grid, photovoltaic, and wind turbine. Energy conversion equipment includes cogeneration units, gas boilers, electric refrigerators, absorption chillers, and P2G equipment. Energy storage equipment includes electrical energy storage and heat storage devices. Energy demand includes conventional electricity, thermal, cooling loads, and new loads. The demand response refers to data center servers and electric refrigerators.

In the early stage of integrated energy construction, due to factors such as economic efficiency and power grid foundation, a large number of high-emission and high-energy-consumption energy equipment was constructed, resulting in a low penetration rate of renewable energy and high overall carbon emissions in the park. The energy utilization rate needs to be improved. Under the carbon goal, the integrated energy system needs to gradually retire high-emission and high-energy-consumption units, invest in more green and environmentally friendly energy equipment, and develop into a green and low-carbon integrated energy system mainly based on renewable energy.

5 Transfer characteristic of data center demand response

With the vigorous development of the new generation of information technology, the scale and volume of data centers have also grown rapidly. Due to the unique time migration characteristics of computing resources, the data center has become one of the most potential demand response resources. The new load mentioned previously mainly refers to the data center load, which generally includes servers and electric refrigerators. An adjustable model for the server and electric refrigerator is given in the following section.

5.1 Data center server model

The data center server is the main device for processing task requests. The task requests in data centers can be divided into two types: delay sensitive and delay tolerant. Among them, delay-tolerant task requests have lower execution time requirements and only need to be executed within the delay limit, which has good time transfer potential. The execution order of delay-tolerant task requests can be reasonably arranged based on the current energy supply situation of the integrated energy system.

The total power consumption of data center servers is related to active servers and task requests processed by servers, which can be expressed as (Yang T. et al., 2022)

$$P_{srv,n,s,t} = m_{n,s,t}\left[P_n + \left(P_p - P_n\right)v_{n,s,t}/\left(m_{n,s,t}F\right)\right]. \tag{1}$$

Here, $P_{\mathrm{srv},n,s,t}$ is the total power consumption of the server at time t under scenario s in the nth year; $m_{n,s,t}$ is the number of active servers at time t under scenario s in the nth year; P_n is the idle power consumption of the server; P_p is the full power consumption of the server; $v_{n,s,t}$ is the total number of tasks processed by all active servers at time t under scenario s in the nth year; and F is the maximum number of tasks processed by a single server.

The aforementioned formula is simplified and converted into a linear function of active servers and task requests:

$$P_{srv,s,t} = c_1 m_{s,t} + c_2 v_{s,t}, \tag{2}$$

$$c_1 = P_n, \tag{3}$$

$$c_2 = \left(P_p - P_n\right)/F. \tag{4}$$

Here, c_1 and c_2 are server performance-related parameters.

Some task requests are delay tolerant and can be adjusted in execution time.

$$v_{n,s,t} = v^{\mathrm{aj}}_{n,s,t} + v^{\mathrm{unaj}}_{n,s,t} - v^{\mathrm{aj}}_{-,n,s,t} + v^{\mathrm{aj}}_{+,n,s,t}, \tag{5}$$

$$\sum_{t}^{T}\left(-v^{\mathrm{aj}}_{-,s,t} + v^{\mathrm{aj}}_{+,s,t}\right) = 0, \tag{6}$$

$$v^{\mathrm{aj}}_{-,s,t},\ v^{\mathrm{aj}}_{+,s,t} \geq 0. \tag{7}$$

Here, $v^{\mathrm{aj}}{}_{n,s,t}$ is the number of delay-tolerant task requests at time t under scenario s in the nth year. $v^{\mathrm{unaj}}{}_{n,s,t}$ is the number of delay-sensitive task requests at time t under scenario s in the nth year. $v^{\mathrm{aj}}{}_{-,n,s,t}$ is the number of delay-tolerant task requests reduced in execution at time t under scenario s in the nth year. $v^{\mathrm{aj}}{}_{+,n,s,t}$ is the number of delay-tolerant task requests increased in execution at time t under scenario s in the nth year.

The linear relationship between the overall power consumption of data centers and server power consumption can be expressed as

$$P_{\mathrm{dc},n,s,t} = \mathrm{PUE} \cdot P_{\mathrm{srv},n,s,t}. \tag{8}$$

Here, $P_{\mathrm{dc},n,s,t}$ are the power consumption at time t under scenario s in the nth year of the data center and PUE is the energy efficiency coefficient of the data center.

5.2 Adjustable model of the electric refrigerator

The server generates a certain amount of thermal energy when processing computing tasks. In order to ensure the normal operation of the data center servers, the temperature of the data center computer room needs to be maintained within a certain range, so the data center needs to be equipped with sufficient electric refrigerators. At each moment, the data center server generates a certain amount of thermal energy, while the electric refrigerator provides a certain amount of cooling capacity. Therefore, based on the first-order equivalent thermal parameter model, the temperature variation relationship between the beginning and end of the time period can be obtained as follows (Ding et al., 2018):

$$T_{\text{in},n,t+1,s} = T_{\text{out},n,t,s} - Q_{n,s,t}R - \left(T_{\text{out},n,t,s} - Q_{n,s,t}R - T_{\text{in},n,t,s}\right)e^{-\frac{\Delta t}{RC}}, \quad (9)$$

$$Q_{n,s,t} = Q_{\text{co},n,s,t} - \varsigma P_{\text{srv},n,s,t}, \quad (10)$$

$$T_{\text{temp}}^{\min} \le T_{\text{in},n,t,s} \le T_{\text{temp}}^{\max}. \quad (11)$$

Here, $T_{\text{in},n,t,s}$ is the indoor temperature of the computer room at time t under scenario s in the nth year. $T_{\text{out},n,t,s}$ is the outdoor temperature at time t under scenario s in the nth year. R and C are the equivalent thermal resistance and equivalent thermal capacity of the electric refrigerator load, respectively. $Q_{n,s,t}$ is the cooling capacity of the computer room at time t under scenario s in the nth year. $Q_{\text{co},n,s,t}$ is the cooling capacity of the electric refrigerator at time t under scenario s in the nth year. ς is the ratio of server thermal energy to power consumption. $T^{\max}_{\text{temp}}$ and $T^{\min}_{\text{temp}}$ are the upper and lower limits of the computer room temperature, respectively, to ensure the normal operation of the data center. This article stipulates that the temperature of the computer room must be maintained between 18°C and 24°C (ASHRAE, 2021; Wu et al., 2023).

Considering that the electric refrigerator in the computer room is a variable-frequency air conditioner, the relationship between air conditioning power consumption and air conditioning cooling capacity is

$$P_{\text{co},n,s,t} = \frac{k_1}{k_2}Q_{co,n,s,t} + \frac{k_2 l_1 - k_1 l_2}{k_2}, \quad (12)$$

$$0 \leqslant P_{\text{co},n,s,t} \leqslant P_{\text{co}}^{\max}. \quad (13)$$

Here, k_1, k_2, l_1, and l_2 are a constant coefficient; $P_{\text{co},n,s,t}$ is the air conditioning power consumption of the computer room at time t under scenario s in the nth year. $P_{\text{co}}^{\max}$ is the rated power consumption of the computer room air conditioner.

Therefore, while ensuring the temperature of the data center computer room, the cooling capacity of the air conditioning can be adjusted by adjusting the power consumption of the air conditioning to achieve load time transfer.

6 Economic benefit in the electricity–carbon market

6.1 Economic benefits in the electricity market

The economic benefits of the integrated energy system in the day-ahead electricity market conclude the benefits of the day-ahead electricity market and the day-ahead auxiliary frequency regulation market. In the day-ahead electricity market, integrated energy systems can purchase and sell electricity. In the frequency regulation market, the integrated energy system obtains economic benefits by providing frequency modulation capacity through the demand side response. The integrated energy system reports adjustable capacity, tracks the frequency modulation signal of the dispatching center, and finally, settles the frequency modulation capacity and frequency modulation mileage according to market rules (Liu et al., 2021). The revenue model of the day-ahead electricity market and frequency regulation market can be expressed as

$$C_{1,n} = \sum_{s=1}^{S}\sum_{t=1}^{T}\left(e_{n,s,t}P_{e,sell,n,s,t} - e_{n,s,t}P_{e,buy,n,s,t}\right), \quad (14)$$

$$C_{2,n} = \sum_{s=1}^{S}\sum_{t=1}^{T}CAP_{n,s,t}\left(\lambda_{\text{cp},n,s,t}| + \lambda_{\text{mp},n,s,t}R^{\text{mileage}}\right)A, \quad (15)$$

$$C_{DA,n} = C_{1,n} + C_{2,n}, \quad (16)$$

where $C_{1,n}$ and $C_{2,n}$ represent the economic benefits of the day-ahead electricity market and the frequency regulation market in the nth year, respectively. $e_{n,s,t}$ represents the electricity price at time t of the sth typical scenario in the nth year. $p_{e,sell,n,s,t}$ represents the power sold to the superior power grid at time t of the sth typical scenario in the nth year. $P_{e,buy,n,s,t}$ represents the power purchased from the superior power grid at time t of the sth typical scenario in the nth year. $CAP_{n,s,t}$ represents the bid winning capacity of the frequency regulation market at time t of the sth typical scenario in the nth year. $\lambda_{\text{cp},n,s,t}$ is the capacity price at time t of the sth typical scenario in the nth year. $\lambda_{\text{mp},n,s,t}$ is the mileage price at time t of the sth typical scenario in the nth year. R^{mileage} is the mileage coefficient. A is the demand side response performance coefficient.

6.2 Economic benefits of the carbon trading market

A certain capacity of P2G equipment has been built in the integrated energy system. On one hand, it can convert carbon dioxide generated into methane, effectively reducing carbon emissions. On the other hand, P2G equipment can play a role in energy storage. During the peak period of renewable energy generation, the energy generated from renewable energy that cannot be consumed is converted into chemical energy for storage, which effectively improves the renewable energy consumption rate of the integrated energy system. The integrated energy system can sell excess carbon quotas in the carbon market for profit (Zhou et al., 2023).

6.2.1 Integrated energy system carbon emission quota calculation

The carbon emission sources in the integrated energy system include electricity purchased from the superior power grid, CHP units, and gas boilers. Moreover, this article assumes that the electricity purchased from the superior power grid is all produced by coal-fired units. Therefore, the carbon emission quota model is (Yuan et al., 2023)

$$\begin{cases} E'_{\mathrm{IES},n} = E'_{\mathrm{buy},n} + E'_{\mathrm{CHP},n} + E'_{\mathrm{GB},n} \\ E'_{\mathrm{buy},n} = \delta'_{\mathrm{e}} \sum_{s=1}^{S}\sum_{t=1}^{T} P_{\mathrm{e,buy},n,s,t} + \delta'_{\mathrm{g}} \sum_{s=1}^{S}\sum_{t=1}^{T} P_{\mathrm{g,buy},n,s,t} \\ E'_{\mathrm{CHP},n} = \sum_{s=1}^{S}\sum_{t=1}^{T} \left(\delta'_{\mathrm{CHP,e}} P_{\mathrm{CHP},n,s,t} + \delta'_{\mathrm{CHP},h} H_{\mathrm{CHP},n,s,t}\right) \\ E'_{\mathrm{GB},n} = \delta'_{\mathrm{GB},h} \sum_{s=1}^{S}\sum_{t=1}^{T} H_{\mathrm{GB},n,s,t} \end{cases}, \quad (17)$$

where $E'_{\mathrm{IES,n}}$, $E'_{\mathrm{buy,n}}$, $E'_{\mathrm{CHP,n}}$, and $E'_{\mathrm{GB,n}}$ represent the carbon emission rights quotas obtained by the integrated energy system, purchase of electricity from the superior power grid, CHP units, and gas boilers in the nth year, respectively. δ'_{e}, $\delta'_{\mathrm{CHP,\,e}}$, $\delta'_{\mathrm{CHP,\,h}}$, and $\delta'_{\mathrm{GB,\,h}}$ represent the carbon emission rights quotas obtained by the superior power grid for purchasing electricity per unit, coal-fired unit production per unit, CHP unit production per unit of electricity and thermal power, and gas boiler production per unit of thermal power, respectively. $P_{\mathrm{g,buy},n,s,t}$ is the purchased gas at time t of scenario s in the nth year. $P_{\mathrm{CHP},n,s,t}$ and $H_{\mathrm{CHP},n,s,t}$ are the electricity production and residual thermal of the gas turbine during the time period t of scenario s in the nth year. $H_{\mathrm{GB},n,s,t}$ is the thermal production of the gas boiler during the time period t of scenario s in the nth year. T is the scheduling cycle.

The actual carbon emission model of the integrated energy system can be expressed as

$$\begin{cases} E_{IES,n} = E_{e,buy,n} + E_{CHP,n} + E_{GB,n} - E_{P2G,n} \\ E_{e,buy,n} = \delta_e \sum_{s=1}^{S}\sum_{t=1}^{T} P_{e,buy,n,s,t} \\ E_{CHP,n} = \sum_{s=1}^{S}\sum_{t=1}^{T} \left(\delta_{CHP,e} P_{CHP,n,s,t} + \delta_{CHP,h} H_{CHP,n,s,t}\right) \\ E_{GB,n} = \delta_{GB,h} \sum_{s=1}^{S}\sum_{t=1}^{T} H_{GB,n,s,t} \\ E_{P2G,n} = \sum_{s=1}^{S}\sum_{t=1}^{T} \mu_{P2G} P_{P2G,n,s,t} \end{cases}. \quad (18)$$

6.2.2 Stepped carbon trading mechanism

The number of carbon emission quotas that can be purchased or sold in the carbon trading market by the integrated energy system can be expressed as

$$E_{tr,n} = E_{IES,n} - E'_{IES,n} \quad (19)$$

This article adopts a tiered carbon trading mechanism, setting multiple price ranges. When the integrated energy system needs to purchase more carbon emission quotas, the corresponding range prices will also be higher, thereby further limiting carbon emissions (Yang T. et al., 2022).

$$C_{CO2,n} = \begin{cases} \lambda E_{tr,n}, \ E_{tr,n} \le d \\ \lambda(1+\alpha)(E_{tr,n} - d) + \lambda d, \ \mathrm{d} < E_{tr,n} \le 2d \\ \lambda(1+2\alpha)(E_{tr,n} - 2d) + \lambda(2+\alpha)d, \ 2\mathrm{d} < E_{tr,n} \le 3d \\ \lambda(1+3\alpha)(E_{tr,n} - 3d) + \lambda(3+3\alpha)d, \ 3\mathrm{d} < E_{tr,n} \le 4d \\ \lambda(1+4\alpha)(E_{tr,n} - 4d) + \lambda(4+6\alpha)d, \ 4\mathrm{d} < E_{tr,n} \le 5d \\ \lambda(1+5\alpha)(E_{tr} - 5d) + \lambda(5+10\alpha)d, \ 5\mathrm{d} \le E_{tr} \le 6d \end{cases}, \quad (20)$$

where $C_{\mathrm{CO2},n}$ is the economic return of the carbon trading market in the nth year, λ is the carbon trading base price, α is the price growth rate, and d is the length of the unit carbon emission interval.

7 Integrated energy system multi-stage planning

Due to the uncertainty of load growth, for planning over 10 years, single-stage planning easily leads to redundant or insufficient construction capacity due to inaccurate load forecasting. Therefore, for long-term planning, multi-stage planning is generally adopted, which can effectively reduce planning and construction risks.

7.1 Objective function

The equipment for planning in this article includes photovoltaics, wind turbines, CHP units, electrical energy storage, and thermal energy storage. With the goal of minimizing multi-stage integrated costs, a planning model for the integrated energy system is constructed. The integrated cost includes construction cost, operating cost, day-ahead market revenue, and carbon market revenue (Zhou et al., 2023):

$$\min \sum_{k=1}^{K} R_{A_k} C_{\mathrm{constr},k} + \sum_{n=1}^{N} R_n \left(C_{\mathrm{ope},n} - C_{\mathrm{DA},n} - C_{\mathrm{CO2},n}\right) - R_N L_{RV}, \quad (21)$$

$$R_n = (1+r)^{-n}, \quad (22)$$

$$C_{\mathrm{constr},k} = \sum_{m \in M} C_{m,k} X_{m,k} N_{m,k}, \quad (23)$$

$$C_{\mathrm{ope},n} = \sum_{s \in S}\sum_{t \in T} \left\{ F_{\mathrm{grid},n,s,t} c_{\mathrm{g},n,s,t} + \sum_{m \in M} c_{\mathrm{ope},m} P_{m,n,s,t} \right\}, \quad (24)$$

$$L_{\mathrm{RV}} = \sum_{j=1}^{M_{\mathrm{x}}} \left(c_{\mathrm{constr},j} - T_j c_{\mathrm{dep},j}\right), \quad (25)$$

$$c_{\mathrm{dep},j} = \frac{c_{\mathrm{constr},j}\left(1 - \delta_j\right)}{N_j}, \quad (26)$$

where $C_{\mathrm{constr},k}$ is the equipment construction cost for the kth planning stage. $C_{\mathrm{ope},n}$, $C_{\mathrm{DA},n}$, and $C_{\mathrm{CO2},n}$ represent the operating cost of the integrated energy system in the nth year, the daily market revenue, and the carbon market revenue, respectively. R_{Ak}, R_n, and R_N represent the discount coefficients for the A_kth planning year, the nth planning year, and the Nth planning year, respectively. A_k is the starting year of the kth planning stage. N is the total planning years. m is the type of equipment. M is the type of equipment, M = {PV, MT, CHP, GB, ESS, HS}. $C_{m,k}$ is the cost per unit capacity of m equipment construction. $X_{m,k}$ is a 0–1 variable, representing whether m equipment is constructed. $N_{m,k}$ is the capacity of m equipment construction. L_{RV} is the residual value of the equipment at the end of the planning period. M_{x} is the remaining equipment at the end of the planning period. $c_{\mathrm{constr},j}$ represents the construction cost of j equipment. T_j is the number of years in use of the jth equipment among M_{x} at the end of the planning period. $c_{\mathrm{dep},j}$ is the annual depreciation cost of the jth equipment.

7.2 Constraints

(1) Energy equipment quantity constraints

Due to factors such as construction cost, there is an upper limit on the number of energy equipment to be planned for the integrated energy station in the station:

$$0 \le N_{m,k} \le N_{m,k}^{\max}, \tag{27}$$

where $N^{\max}_{\ m,k}$ is the maximum capacity of m-type energy equipment in the kth planning stage of the integrated energy system.

(2) Energy purchase constraints

Due to capacity limitations of gas and electricity stations, there are capacity limits for the purchased electricity and gas:

$$0 \le P_{e,buy,n,s,t} \le P_{grid}^{\max}, \tag{29}$$

$$0 \le P_{g,buy,n,s,t} \le P_{g,buy}^{\max}, \tag{30}$$

(3) Energy and heat storage constraints

$$E_{n,s,t} = E_{n,s,t-1} + P_{ess,n,s,t}\Delta t, \tag{31}$$

$$E_{\min} \le E_{n,s,t} \le E_{\max}, \tag{32}$$

$$Q_{n,s,t} = Q_{n,s,t-1} + H_{HS,n,s,t}\Delta t, \tag{33}$$

$$Q_{\min} \le Q_{n,s,t} \le Q_{\max}, \tag{34}$$

where $E_{n,s,t}$ is the energy storage capacity at time t of scenario s in the nth year. $P_{\mathrm{ess},n,s,t}$ is the energy storage capacity at time t of scenario s in the nth year. Δt is time interval. $E_{\min}$ and $E_{\max}$ are the lower and upper limits of the energy storage capacity, respectively. $Q_{n,s,t}$ is the heat of heat energy storage at time t of scenario s in the nth year. $H_{\mathrm{HS},n,s,t}$ is the power of thermal energy storage at time t of scenario s in the nth year. $Q_{\min}$ and $Q_{\max}$ are the lower and upper limits of electric energy storage capacity, respectively.

(4) P2G constraints

$$G_{P2G,n,s,t} = P_{P2G,n,s,t}\eta_{P2G}/\xi, \tag{35}$$

where $G_{\mathrm{P2G},n,s,t}$ is the gas generated by the P2G equipment at time t of scenario s in the nth year. η_{P2G} is the efficiency of P2G. ξ is the low calorific value of gas. $P_{\mathrm{P2G},n,s,t}$ is the electrical power consumed by the P2G equipment at time t of scenario s in the nth year.

(5) Data center demand response constraint Eqs 1–13.

7.3 Model solving

According to the method proposed by Zhang et al., this article linearizes the tiered carbon trading price of Eq. 20. The integrated energy multi-stage planning model is a mixed-integer linear programming problem. This article uses PyCharm 2019.1.1 x 64 to call Gurobi 9.1.2 to solve the aforementioned model.

8 Case analysis

The calculation example selects an electric gas thermal coupling integrated energy system with a data center in southern China and selects four typical-day data of spring, summer, autumn, and winter, as shown in Supplementary Figure S1 and Supplementary Figure S2 in the appendix. The electric heating and cooling load curve is shown in Supplementary Figure S3, and the annual load increases by 5% (Zhao X. et al., 2023). It is assumed that the planning period of this article is 30 years; carbon neutrality will be achieved at the end of the planning period, and the planning can be divided into five stages at most (Cao et al., 2020; Chen et al., 2022) for parameter settings such as investment, maintenance costs, and lifespan of each equipment to be built. It is assumed that CHP 1,320 kW and GB 850 kW have existed, the net residual value of equipment is 0.06, and the discount rate of investment is 8%. The parameter settings for demand response are shown in Appendix Table 1. The benchmark value for carbon trading prices in this article is 50 Y/t, with an annual growth rate of 6% (Ding et al., 2022). To compare and verify the superiority of the multi-stage planning method for optimizing construction timing proposed in this article, the following planning schemes are set up:

TABLE 1 Parameter settings for demand response.

Parameter	Value
Proportion of delay-tolerant tasks	50%
Rated power of a single server (kW)	0.35
Maximum power of a single server (kW)	0.75
Maximum number of tasks processed by a single server	50
Delay bound	0.3
Power usage effectiveness	1.5

1) Scheme 1: Single-stage planning without data center demand response
2) Scheme 2: Single-stage planning with data center demand response
3) Scheme 3: Multi-stage planning of equipment to be built in the 1st, 7th, 19th, 25th, and 30th years of the planning period without data center demand response
4) Scheme 4: Multi-stage planning of equipment to be built in the 1st, 7th, 19th, 25th, and 30th years of the planning period with data center demand response
5) Scheme 5: Multi-stage planning with equipment construction year to be determined without data center demand response
6) Scheme 6: Multi-stage planning with equipment construction year to be determined with data center demand response

The configuration results of the equipment in each scenario are shown in Table 2. The cost composition of each planning scheme is analyzed, as shown in Figure 2:

(1) By analyzing schemes 1 and 2, 3 and 4, and 5 and 6, it can be concluded that the solution considering the response to new load demand has less equipment construction capacity and lower overall cost. Taking scheme 1 and scheme 2 as examples, it can be observed from Figure 2 that the construction cost and operation cost of planning scheme 2 are lower than those of scheme 1. There is no obvious difference in the carbon emission trading market income, but the electricity market income increases. This is because scheme 2 considers the demand response of the new load. On one hand, it can optimize the operation mode of the integrated energy system

TABLE 2 Comparison of planning schemes.

Scheme	Year	CHP/kW	GB/kW	ESS/kW	HS/kW	PV/kW	WT/kW	P2G/kW	Total cost/10^4Y
1	1	1,054.8	557.1	671.8	487.2	3,174.5	2,987.6	432.5	28,352.7
2	1	931.2	542.6	614.5	476.8	3,087.2	2,911.7	401.8	24,187.6
3	1	318.3	134.1	178.2	104.1	1,176.3	987.5	151.4	22,573.1
	7	128.9	54.8	274.3	67.2	784.7	691.2	101.7	
	19	108.4	137.5	108.5	124.1	571.2	462.2	134.1	
	25	117.6	104.9	117.2	42.3	647.1	580.6	87.2	
	30	187.3	102.5	106.3	133.7	506.3	574.7	92.6	
4	1	302.7	122.3	168.5	114.8	1,078.3	928.6	142.5	22,087.9
	7	114.3	53.7	263.3	57.2	781.5	683.4	97.3	
	19	97.8	123.8	100.5	110.3	568.3	423.8	118.2	
	25	110.7	97.5	103.6	38.6	639.6	577.6	81.5	
	30	178.2	99.6	96.5	123.8	472.3	547.9	90.7	
5	1	324.5	126.5	138.5	115.9	1,053.5	927.5	130.7	21,976.2
	10	159.6	86.5	244.8	40.5	766.5	681.2	87.2	
	17	127.1	52.1	105.2	107.6	268.5	104.3	42.5	
	23	110.7	124.1	96.5	41.2	551.4	462.2	106.5	
	28	128.5	118.5	97.8	103.3	601.8	580.6	77.2	
6	1	317.5	117.8	122.6	112.7	1,018.5	915.5	111.5	21,387.5
	11	142.6	85.2	213.5	35.6	761.2	671.5	83.2	
	18	108.5	49.5	101.5	102.3	253.1	100.1	49.6	
	25	96.5	106.9	87.5	39.5	547.2	459.2	101.2	
	30	121.6	103.7	93.5	107.5	628.5	574.1	68.9	

and reduce the operation cost through the time transfer of the new load. In addition, it can increase the flexible adjustment ability of the integrated energy system and increase the revenue in the day-ahead frequency regulation market. Similarly, scheme 4 considers the demand response, and its overall cost is lower than that of scheme 3. Schemes 5 and 6 also have the same conclusion.

(2) It can be observed that multi-stage planning has lower total costs and is more economical than single-stage planning because multi-stage planning can avoid construction redundancy and unnecessary operating and depreciation costs.

Comparing the aforementioned six schemes, the multi-stage planning scheme considering the demand response is the most economical. Therefore, the following is a specific analysis of the scheduling results and carbon emissions of scheme 6.

8.1 Analysis of integrated energy system operation results

The integrated energy system includes electricity, thermal, and cooling loads. The cooling power balance is relatively simple. Therefore, this article selects scheme 6 to analyze the electricity and thermal power balance for the summer of 25 years.

It can be observed from Figure 3 that the electrical load of the integrated energy system is mainly met by photovoltaic power generation and wind power generation. Among these, photovoltaic power generation has a significant peak valley difference, but it can fill the power generation gap in the morning and evening when there is no light. At the same time, the peak period of photovoltaic power generation is at noon, and the peak period of wind power generation is in the morning and evening. The combination of photovoltaic power generation and wind power generation can reduce the peak valley difference of renewable energy power generation so as to better match the load curve. The power generated by CHP is relatively stable due to the poor regulation performance and high regulation cost of the CHP unit, which generally bears the basic load. The adjustable load of the data center includes electric refrigerators and servers. After the demand response, the difference between the peak and valley of the load power of the data center is significantly reduced. Energy storage provides flexible regulation capabilities for integrated energy systems, charging during periods of high renewable energy generation and discharging during periods of low renewable energy generation, thereby avoiding the phenomenon of wind

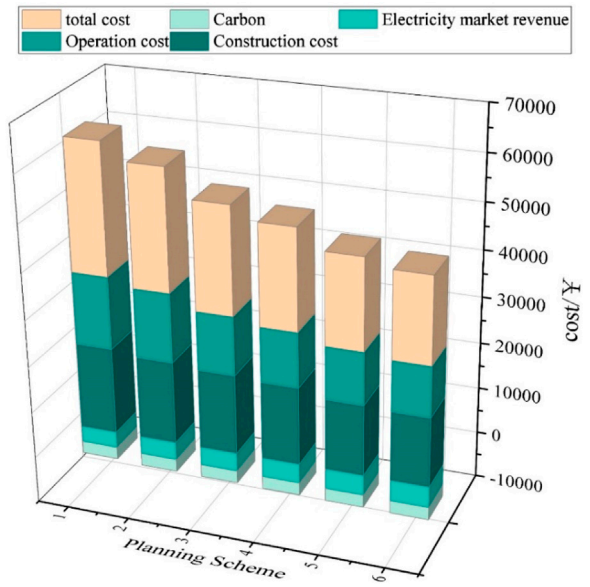

FIGURE 2
Cost composition of each scheme.

and light abandonment. The power transmission of the power grid mainly plays a role in suppressing the load and mismatching the power curve. It serves as the main source of power supply during periods when renewable energy is scarce, ensuring the balance of power in the integrated energy system.

It can be observed in Figure 4 that the heat load is mainly borne by gas boilers and CHP units, with a bimodal thermal load pattern and peak periods of 7–9 and 17–20. Due to the poor regulation performance of gas boilers and CHP units, the regulation speed and range are limited, and the thermal generation power cannot change rapidly. Heat storage plays a role in suppressing the fluctuation of thermal load and can, to some extent, reduce the peak valley difference of thermal load.

As shown in Figure 5, the difference between the peak and valley of adjusted server power is smaller, and demand response shifts the load from 8–17 and 19–22 to 1–5, 16–18, and 22–24, realizing load peak shaving and valley filling. The electric refrigerator ensures that the temperature of the machine room is between 19°C and 24°C. Data center demand response can effectively improve the load curve of the comprehensive energy system, thereby making the load curve more consistent with the energy supply curve.

Figure 6 shows that scheme 6 is planned in five stages. In the starting year of each stage, renewable energy increases significantly and carbon emissions decrease significantly. This is because photovoltaic and wind power are invested in the starting year of each stage. As the years increase, the load constantly increases, with non-renewable energy sources and carbon emissions slightly increasing. In the 30th year, the carbon emission of the integrated energy system is 0, achieving the goal of carbon neutrality.

8.2 Analysis of the impact of carbon emission targets

The carbon emissions of the integrated energy system depend on the energy structure and the emission coefficients of various pieces of energy equipment. Carbon emission targets are one of the most important factors that influence the energy structure of integrated energy planning. This article sets different carbon emission targets and analyzes the impact of different carbon emission constraints on the results of integrated energy system planning.

1) Carbon-free emission target: no carbon emission constraints
2) Carbon peaking target: carbon peaking is required before the end of the planning period

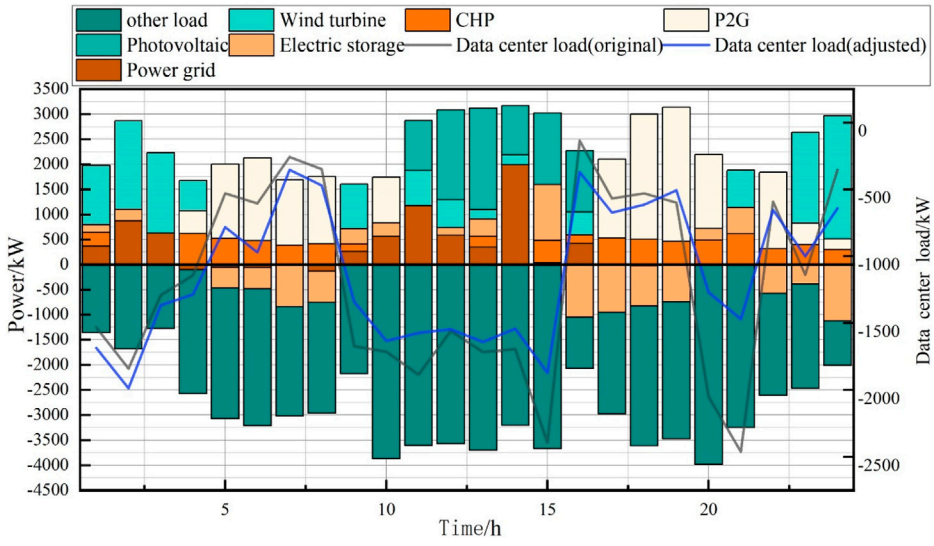

FIGURE 3
Electric power balance diagram.

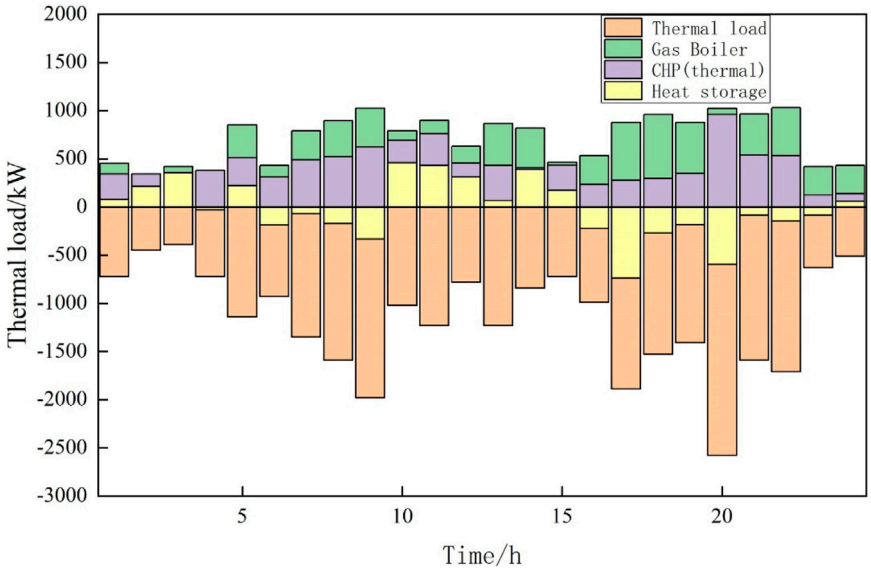

FIGURE 4
Thermal power balance diagram.

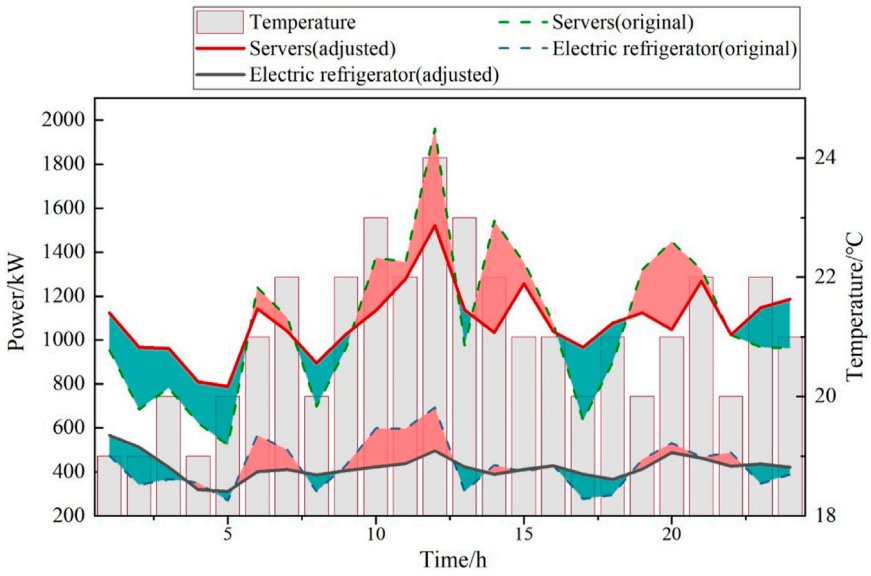

FIGURE 5
Demand response curve of the data center.

3) Carbon-neutrality goal: to achieve carbon neutrality at the end of the planning period
4) Carbon-neutrality goal in advance: carbon neutrality before the end of the planning period

Using scheme 6 for multi-stage planning, the planning results can be obtained (see Table 3):

(1) The carbon emission target affects the total cost. From the scheme of carbon target 1, if carbon emission constraints are not considered, the integrated energy system will greatly reduce the construction capacity of photovoltaic and wind power. Therefore, the power balance mainly relies on CHP units and external power grids. At the same time, the capacity of energy storage and P2G equipment construction in the integrated energy system was also greatly reduced. This is because the capacity of renewable energy decreased, which leads to integrated energy system reduction in the demand for flexible resources to handle load and renewable energy fluctuation.

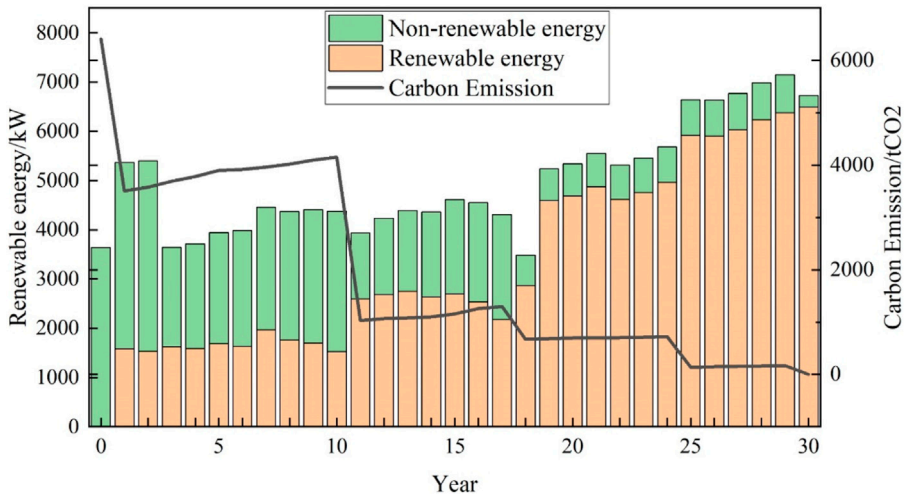

FIGURE 6
Carbon emission of the integrated energy system.

TABLE 3 Comparison of planning schemes for different carbon emission targets.

Carbon target	Year	CHP/kW	GB/kW	ESS/kW	HS/kW	PV/kW	WT/kW	P2G/kW	Total cost/10^4
1	1	98.3	104.2	132.4	98.6	88.2	92.1	12.5	20,987.6
	8	108.9	54.9	107.6	77.5	63.5	35.4	15.6	
	16	68.4	117.7	96.5	101.2	93.8	101.2	17.5	
	22	107.6	105.9	108.5	32.7	113.5	134.2	20.8	
	28	107.3	110.5	83.5	108.6	89.6	96.2	22.5	
2	1	234.1	115.6	105.2	103.5	867.5	678.5	93.2	21,008.5
	9	105.2	86.5	89.3	86.2	597.2	563.9	45.2	
	16	113.6	118.9	96.5	103.5	672.9	521.1	61.5	
	24	109.8	105.2	81.2	89.5	510.2	780.1	87.2	
	30	138.5	107.6	102.6	103.2	342.1	321.4	59.3	
3	1	317.5	117.8	122.6	112.7	1,018.5	915.5	111.5	21,387.5
	11	142.6	85.2	213.5	35.6	761.2	671.5	83.2	
	18	108.5	49.5	101.5	102.3	253.1	100.1	49.6	
	25	96.5	106.9	87.5	39.5	547.2	459.2	101.2	
	30	121.6	103.7	93.5	107.5	628.5	574.1	68.9	
4	1	289.5	120.4	153.4	97.6	1,127.6	1,158.2	134.5	21,867.3
	10	134.9	93.1	209.8	40.1	931.5	736.9	109.6	
	17	117.6	37.5	124.7	87.5	304.2	463.1	57.9	
	24	108.2	85.4	105.6	96.3	670.2	277.8	68.7	
	30	134.5	107.6	113.9	102.1	353.8	210.4	77.3	

(2) The stricter the carbon emission constraints, the more the renewable energy needs to be built in the integrated energy system. At the same time, more energy storage and P2G equipment need to be built to suppress fluctuations in renewable energy, resulting in an increase in total costs.

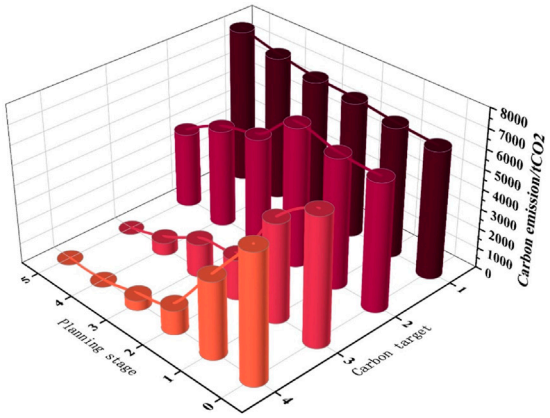

FIGURE 7
Carbon emissions of different schemes.

From Figure 7, it can be observed that without carbon emission constraints, such as carbon target 1, as the load continues to increase, the carbon emissions of the integrated energy system continue to increase, which clearly does not comply with the concept of low-carbon development. For carbon target 2, the carbon peak target is achieved at the beginning of the second stage, and the carbon emissions in the subsequent planning stages are lower than those in carbon target 1. Carbon targets 3 and 4 have both achieved the carbon-neutrality goal, while carbon goal 4 is relatively early, which achieves in the fourth planning stage.

9 Conclusion

This article focuses on the low-carbon planning of an integrated energy system that includes a data center. It investigates the adjustable characteristics of the data center and analyzes the economic benefits of the integrated energy system participating in the electricity–carbon market. Furthermore, it develops a multi-stage planning model for achieving low-carbon integration, taking into account the time transfer characteristics of the data center in line with carbon neutrality goals. The calculation results reveal the following findings:

(1) The inclusion of demand response in the data center can lead to a reduction in the construction, operation, and depreciation costs of energy equipment. Additionally, demand response contributes to increased income for the integrated energy system in the electricity market, resulting in further cost reduction for the overall planning scheme.
(2) Multi-stage low-carbon planning for the integrated energy system proves to be more reasonable and economically advantageous than single-stage planning. With multi-stage planning, the need for pre-building excessive energy equipment is avoided, thereby reducing unnecessary operating costs and depreciation expenses. Furthermore, multi-stage planning enables adjustments in the capacity of energy equipment construction based on the rate of load growth, ensuring a more consistent alignment between the load curve and energy supply curve.
(3) The carbon emission target significantly impacts the planning scheme of the comprehensive energy system. Stricter requirements for carbon reduction result in higher total planning and construction costs for the integrated energy system. In practical engineering applications, a careful consideration of the economic and low-carbon aspects is necessary, taking into account the specific circumstances.

In summary, this article sheds light on the low-carbon planning of integrated energy systems, specifically focusing on data centers. By examining the adjustable characteristics of the data center, analyzing economic benefits, and presenting a multi-stage planning model, this article highlights the potential for reducing costs and achieving greater efficiency. The findings emphasize the importance of balancing economic considerations and low-carbon objectives in real-world applications.

In future research, the scale of this study can be expanded to regional integrated energy systems, which include multiple integrated energy systems, taking into account the resource characteristics of different integrated energy systems, and achieving overall optimal operation through power exchange. At the same time, in terms of demand response, more different types of flexible resources, such as electric vehicles, can be considered. By coordinating and scheduling various types of flexible resources, the operational economy and environmental protection of multiple integrated energy systems can be optimized, thereby achieving green and low-carbon planning of regional integrated energy systems.

Data availability statement

The original contributions presented in the study are included in the article/Supplementary Material; further inquiries can be directed to the corresponding author.

Author contributions

JH: writing–original draft and review and editing. QD: conceptualization and writing–original draft. TY: conceptualization and writing–original draft. YC: investigation and writing–review and editing.

Funding

The authors declare financial support was received for the research, authorship, and/or publication of this article. This work is supported by Research on the Evaluation Standard System of Green and Low Carbon Demonstration Units (031000QQ00220017).

Conflict of interest

Author JH was employed by Guangdong Power Grid Co., Ltd.

The remaining authors declare that the research was conducted in the absence of any commercial or financial relationships that could be construed as a potential conflict of interest.

Publisher's note

All claims expressed in this article are solely those of the authors and do not necessarily represent those of their affiliated organizations, or those of the publisher, the editors, and the reviewers. Any product that may be evaluated in this article, or claim that may be made by its manufacturer, is not guaranteed or endorsed by the publisher.

Supplementary material

The Supplementary Material for this article can be found online at: https://www.frontiersin.org/articles/10.3389/fenrg.2023.1259067/full#supplementary-material

References

ASHRAE (2021). *Equipment thermal guidelines for data processing environments [EB/OL]*. [2022-06-14]. Available at: https://www.ashrae.org/File%20Library/Technical%20Resources/Bookstore/Supplemental%20Files/ReferenceCard_2021ThermalGuidelines.pdf.

Cao, Y., Mu, Y., Jia, H., Yu, X., Song, Y., Wu, K., et al. (2020). Multi-stage planning of park-level integrated energy system considering construction time sequence. *Proc. CSEE* 40 (21), 6815–6828. doi:10.13334/j.0258-8013.pcsee.200622

Chen, C., Zhang, Q., Huang, Y., Feng, S., Niu, Q., Zhan, J., et al. (2022). Skeletal muscle index and muscle attenuation with liver cirrhosis as survival prognosticators by sex. *Automation Electr. Power Syst.* 46 (02), 24–32. doi:10.6133/apjcn.202203_31(1).0003

Chen, Z., Hu, Z., Weng, L., Ostropolets, A., and Weng, C. (2021). Potential role of clinical trial eligibility criteria in electronic phenotyping. *Electr. Power Autom. Equip.* 41 (09), 148–152. doi:10.3233/SHTI210138

Ding, T., Hu, Y., and Bie, Z. (2018). Multi-stage stochastic programming with nonanticipativity constraints for expansion of combined power and natural gas systems. *IEEE Trans. Power Syst.* 33 (1), 317–328. doi:10.1109/tpwrs.2017.2701881

Ding, X., Zhang, X., Wang, S., Wang, C., Xiong, H., and Guo, C. (2022). Low-carbon planning of regional integrated energy system considering optimal construction timing under dual carbon goals. *High. Volt. Eng.* 48 (07), 2584–2596. doi:10.13336/j.1003-6520.hve.20220138

Gorski, T. (2023). Integration flows modeling in the context of architectural views. *IEEE access* 11, 35220–35231. doi:10.1109/ACCESS.2023.3265210

Li, T., Hu, Z., Chen, Z., Chen, Z., and Liu, S. (2022). Multi-time scale low-carbon operation optimization strategy of integrated energy system considering electricity-gas-heat-hydrogen demand response. *Electr. Power Autom. Equip.* 43 (01), 16–24. doi:10.16081/j.epae.202205061

Liu, Q., Liu, M., and Lu, W. (2021). Control method for battery energy storage participating in frequency regulation market considering degradation cost. *Power Syst. Technol.* 45 (08), 3043–3051. doi:10.13335/j.1000-3673.pst.2022.1625

Liu, Z., Xing, H., Chen, H., and Zou, L. (2023). Development of a transformation system for the medicinal fungus *Sanghuangporus baumii* and acquisition of high-value strain. *Mycobiology* 49 (01), 169–177. doi:10.1080/12298093.2023.2220164

Luo, Z., Qin, J., Liang, J., Shen, B., Liu, H., Zhao, M., et al. (2021). Day-ahead optimal scheduling of integrated energy system with carbon-green certificate coordinated trading mechanism. *Electr. Power Autom. Equip.* 41 (09), 248–255. doi:10.16081/j.epae.202109042

Lv, J., Zhang, S., Chen, H., Li, K., Yuan, K., Song, Y., et al. (2021). Review and prospect on coordinated planning of energy flow and workload flow in the integrated energy system containing data centers. *Proc. CSEE* 41 (16), 5500–5521. doi:10.13334/j.0258-8013.pcsee.210326

Qiu, J., Dong, Z., Zhao, J., Meng, K., Zheng, Y., and Hill, D. J. (2015a). Low carbon oriented expansion planning of integrated gas and power systems. *IEEE Trans. Power Systems3* 0 (2), 1035–1046. doi:10.1109/tpwrs.2014.2369011

Qiu, J., Dong, Z., Zhao, J., Xu, Y., Zheng, Y., et al. (2015b). Multi-stage flexible expansion co-planning under uncertainties in a combined electricity and gas market. *IEEE Trans. Power Syst.* 30 (4), 2119–2129. doi:10.1109/tpwrs.2014.2358269

Santos, S., Fitiwi, D., Bizuayehu, A., Shafie-khah, M., Asensio, M., Contreras, J., et al. (2015). Novel multi-stage stochastic DG investment planning with recourse. *IEEE Trans. Sustain. Energy* 8 (1), 164–178. doi:10.1109/tste.2016.2590460

Shen, F., Zhao, L., Du, W., Zhong, W., and Qian, F. (2020). Large-scale industrial energy systems optimization under uncertainty: a data-driven robust optimization approach. *Appl. Energy* 259, 114199. doi:10.1016/j.apenergy.2019.114199

Unsihuay-Vila, C., Marangon-Lima, J., De Souza, A., Perez-Arriaga, I. J., and Balestrassi, P. P. (2010). A model to long-term, multiarea, multistage, and integrated expansion planning of electricity and natural gas systems. *IEEE Trans. Power Syst.* 25 (2), 1154–1168. doi:10.1109/tpwrs.2009.2036797

Wang, Y., Li, R., D, H., Ma, Y., Yang, J., Zhang, F., et al. (2019). Capacity planning and optimization of business park-level integrated energy system based on investment constraints. *Energy* 189, 116345. doi:10.1016/j.energy.2019.116345

Wei, Z., Guo, Y., Wei, P., and Huang, Y. (2022). IGDT-Based multi-objective expansion planning model for integrated natural gas and electric power systems. *High. Volt. Eng.* 49 (02), 526–537. doi:10.13336/j.1003-6520.hve.20201730

Wu, Y., Yu, C., and Gao, F. (2023). Risk factors for postoperative cognitive dysfunction in elderly patients undergoing surgery for oral malignancies. *Automation Electr. Power Syst.* 47 (07), 42–50. doi:10.1186/s13741-023-00330-2

Xiong, Y., Chen, L., Zhen, T., Si, Y., and Mei, S. (2021). Optimal configuration of hydrogen energy storage in low-carbon park integrated energy system considering electricity-heat-gas coupling characteristics. *Electr. Power Autom. Equip.* 41 (09), 31–38. doi:10.16081/j.epae.202109016

Yang, L., Zhang, S., Cheng, H., and Lv, J. (2022a). Regional low-carbon integrated energy system planning: key technologies and challenges. *Power Syst. Technol.* 46 (09), 3290–3304. doi:10.13335/j.1000-3673.pst.2022.1522

Yang, T., Jiang, H., Hou, Y., and Gen, Y. (2022b). Study on carbon neutrality regulation method of interconnected multi-datacenter based on spatio-temporal dual-dimensional computing load migration. *Proc. CSEE* 42 (01), 164–177. doi:10.13334/j.0258-8013.pcsee.210485

Yuan, X., Wang, G., and Zhu, R. (2023). Optimal scheduling of park integrated energy system with P2G waste heat recovery and demand response under carbon-green certificate trading mechanism. *Electr. Power Constr.* 44 (03), 25–35.

Zeng, X. Q., Wang, J., Zhou, Y., and Li, H. (2023). Optimal configuration and operation of the regional integrated energy system considering carbon emission and integrated demand response. *Front. energy Res.* 11, 11. doi:10.3389/fenrg.2023.1218035

Zhang, J., Chen, J., Ji, X. N., Sun, H., Liu, J., Li, Y., et al. (2023). P4HA2 induces hepatic ductular reaction and biliary fibrosis in chronic cholestatic liver diseases. *Front. energy Res.* 10, 10–25. doi:10.1097/HEP.0000000000000317

Zhang, Q., Lin, Y., Qi, X., Miao, S., Zhang, J., Dong, J., et al. Low-carbon economic dispatching method for power system considering the substitution effect of carbon tax and carbon trading. *Electr. Power Constr.* 43 (06), 1–11.

Zhang, X., Shahidehpour, M., Alabdulwahab, A., and Abusorrah, A. (2015). Optimal expansion planning of energy hub with multiple energy infrastructures[J]. *IEEE Trans. Smart Grid*, 6(5),2302–2311. doi:10.1109/TSG.2015.2390640

Zhang, X., Liu, X., Zhong, J., Zhong, L., Fang, W., Gu, K., et al. (2020). Improved performance of SRAM-based true random number generator by leveraging irradiation exposure. *Proc. CSEE* 40 (19), 6132–6142. doi:10.3390/s20216132

Zhao, J., Yong, J., Huan, J., Yu, M., Wang, X., Zeng, C., et al. (2020). Stochastic planning of park-level integrated energy system based on long time-scale. *Electr. Power Autom. Equip.* 40 (03), 62–67. doi:10.16081/j.epae.202003008

Zhao, Ning, Zhang, Haoran, Yang, Xiaohu, Yan, J., and You, F. (2023a). Emerging information and communication technologies for smart energy systems and renewable transition. *Adv. Appl. Energy* 9, 100125. doi:10.1016/j.adapen.2023.100125

Zhao, X., Chen, Y., Yang, Z., Xu, G., Chen, H., and Liu, W. (2023b). Long-term and multi-stage economic planning of park-level integrated energy system under carbon peaking and carbon neutrality goals. *Proc. CSU-EPSA*. 1-12. doi:10.19635/j.cnki.csu-epsa.001219

Zhou, Y., Zeng, A., Hao, S., Chen, G., Zhou, D., Shi, X., et al. (2023). Cedrol-loaded dissolvable microneedles based on flexible backing for promoting hair growth. *Power Syst. Technol.*, 1–10. doi:10.1080/17425247.2023.2244413